STRESS CONCENTRATION FREE SPLINE FOR HIGH TORQUE TWIN SCREW POWER TRANSMISSION

Joe Mattingly, SteerAmerica Inc., Uniontown, OH
Dr. Babu Padmanabhan, C.J. Chetan, Steer Engineering Pvt. Ltd., Bangalore, India

Abstract

Torque transmission between a shaft and a driven member requires a key-way or the use of integral "splined" shafts. Co-rotating twin-screw extruders are designed with "extreme" engineering requirements due to the close center distance of operation between the two working shafts. A study of involute vs. continua spline applications (based on the cycloidal displacement curve) on the thin walled torque transmitting components using mathematical, and FEM analysis, predicts a marked decrease in the stress concentration factor for continua splines. Physical testing confirms that the decrease in stress concentration translates to a marked increase in torque transmission capability in thin walled torque transmission components.

Introduction

Traditionally, involute splined shafts were designed for transmitting torque to "thick-walled" hubs, gears, pulleys, and sprockets. Co-rotating twin-screw extruders are designed with "extreme" engineering requirements due to the close center distance of operation between the two working shafts. As a result thin-walled torque transmitting components have to be used. Over the years several designs have evolved to utilize in the thin walled extrusion applications, this includes straight sided spline and 20 and 30 degree pressure angle involute splines. There are no international standards to address the issues with respect to thin walled components and many manufacturers are resorting to sub-optimal non standard design.

During power transmission spline like gear teeth are subjected to stresses in bending, shear, compressive and contact loads. Dudley [1] found that in failure the spline gets fractured as a cantilever type beam. Burke and Fischer [2] found through experiments that the spline experiences extremely complex and interacting stresses. Salyards and Macke [3] found in Photoelastic studies that the stress at the tooth fillet was the dominant component. However, they found that the stress was not only due to pure bending, but also due to Hoop stress, Torsional stress, and Contact stress.

Each tooth can be considered as an inclined cantilever beam Dudley [4]. Force acting on each tooth can be resolved into a tangential (F_t) and the radial component (F_r) (Fig. 1). In the present case only bending and axial stresses are discussed.

Dudley [3] has applied this general equation to gear teeth to the maximum tooth stress.

$$(\text{Maximum stress})_{Ft} = (6*Ft*L*Kf)/(t_b^2*L) \quad (1)$$

As evidenced from Equation (1) the magnitude of the stress induced increases with the increase in the stress concentration factor Kf. Dolan and Broghamer [5] performed numerous photoelastic experiments and developed the following relationship for Kf.

$$Kf = H+\{t_b/r\}^N *\{t_b/L\}^M \quad (2)$$

Where: r is the radius of the tooth fillet,
t_b is the tooth thickness at the base of the spline that is considered the beam:
$H = 0.331-0.436Ø$ (3)
$M = 0.261-0.545Ø$
$N = 0.324-0.492Ø$
And Ø = the pressure angle in radians

The radial force component induces compressive stress. This compressive stress is uniformly distributed along the cross section of the beam (every tooth is a beam) and is defined in Equation (4).

$$\text{Stress due to the Radial component} = Fr/(L* t_b) \quad (4)$$

When equations 2 and 3 were used to find the stress concentration factor in involute (30º pressure angle) and Continua spline (40º pressure angle), the stress concentration factor was 1.28 and in continua 0.9 (see appendix A)

Additionally finite element analysis of an involute spline was reviewed (as it is in Abstract) [8]. Two finite element analysis of an involute spline are performed; one is asymmetrical loaded and the other is non-asymmetrical loaded. An entire cross section of both an internal and external pair is analyzed for both models. It is shown that

on the asymmetrically loaded spline the highest stress experienced is the maximum compressive contact stress although the tensile stress in the shaft is also quite high. It is also shown that stress concentrations exist at the root and top of the tooth for both models. Furthermore, on the non-asymmetrical loaded spline at low, more teeth come in contact. All the stresses remain relatively constant under increasing torque as more teeth are engaged. Once all teeth are in contact stress increases with higher torques. However, the maximum tensile stress (arising from stress concentrations) remains fairly constant, even at high torques, because the stress concentrations that occur at tooth roots appear to be relatively independent of the number of teeth in contact.

.Figure 2, shows the stress distribution in involute splines when subjected to torsion. The red color indicates the highest levels of stress. STEER's FEM analysis (using ANSYS 10) of the continua splines, clearly show there is no observable evidence of stress concentration at the base of the spline in comparison with the involute spline (Fig. 3).

Our study additionally looks at an actual performance comparison of the involute vs. the continua spline in the use of thin walled power transmission components.

Experimental

Experimental investigations were carried out using a Torsional Test Rig (Fig. 4) to compare the load bearing capacity of involute and Continua splines. Our Torsional Test Rig (TTR), tested bushings with both involute and continua splines with identical wall thicknesses, along with shafts with Continua and Involute splines. We utilized 50 mm bushings that act as a coupling between two shafts. The shafts are made of AISI H13, a Molybdenum Hot Work Tool Steel. The shafts were hardened and tempered to a hardness of 52+/- 3 RC. The required splines were generated on all shafts and bushings. The Bushings are made of STEER's Material grades. The splines were generated using CNC W/C EDM. The pieces were then subject to grit blasting to overcome residual tensile stresses. Each shaft was designed to mesh with a 20 mm length of the bushing's internal profile (Fig. 5)

In the TTR, one end of the shaft is fixed and the other end is subjected to torsional load. (Fig. 6) The degree of twisting of the shaft was increased until a permanent shear deformation or fracture occurred in the bushing which was acting on the coupling. The torque induced at the fracture point was then recorded.

The load bearing capacities in torsion of the identical number (24) of involute and continua splines is shown. (Fig. 7) The results plotted are modal value approximations. This is done for the material defect rectification. As evidenced by Fig. 7 the Continua splined bushing has double the torque capacity when compared to involute spline.

Results and Discussion

Torque at the failure point for continua splines was recorded at 1000 Nm versus 500 Nm for involute splines on the same test apparatus. .It should be noted that the experimental results do not match the predicted mathematical Kf, value result, but approximate a Kf value of nearly 3x of that predicted for the involute spline. The continua spline morphology is made with a single curve with continuity unlike that of the involute with discontinuity (Fig.8). This discontinuity has created an opportunity for stress concentration at these points. The performance comparison of the involute vs. the continua spline in the use of thin walled power transmission components reveals the critical nature and complexity of the spline design in thin walled applications.

Conclusions

An experimental investigation was conducted to investigate the torque load carrying capacity of involute and continua splines in a thin walled application. A Twenty four spline configuration was used in both continua and involute shafts and bushings. The relative stress concentration was evaluated both qualitatively, in terms of physical performance on the TTR, as well as quantitatively, by FEM and mathematical analysis for the stress concentration factor. Experimentally observed results showed that the continua splined bushing and screw shaft out performed the involute bushing and screw shaft. It is evident that the stress concentration factor in the involute splines resulted in a lower torque capacity compared to that of the continua splines. It is also evident from the literature that the stress concentration factor affects the torque capacity to a great extent.

References

1. Dudley D.W., "How Splines Need Stress Control", Product Engineering, December 23, 1957, pp 56-61.
2. Burke, P.E. and Fischer, W., "Design and Analysis Procedures for Shafts and Splines", SAE Technical Paper 680024, 1968.
3. Salyards, D.G. and Macke, H.J., "The Application of Photoelasticity to the Analysis of Shaft Splines", Proceedings of the 1990 SEM Spring Conference of Experimental Mechanics; Albuquerque, New Mexico, June 4-6, 1990.
4. Dudley D.W., Dudley's Gear Hand Book. 2nd Edition, McGraw-Hill, Inc., 1991.

5. Dolan, T.J. and Broghammer, E.L., “A Photoelastic Study Of Stresses in Gear Tooth Fillets.” Report No.335, Univ. of Illinois Engineering Experiment Station, March 1942.
6. Brian J.K.De Caires., “Variation of Involute Spline Tooth Contact’, A Master Thesis from Brigham Young University.
7. Donald Alexander Baker, A Finite Element Study of Stress in Splined and Partially Splines Shafts under Bending, Torsion, and Combined Loading”, A Master Thesis from Virginia Tech.
8. Zella L. Kahn-Jetter and Suzanne Wright, Journal Of Mechanical Design—June 2000—Volume 122, Issue 2, pp. 239-244.

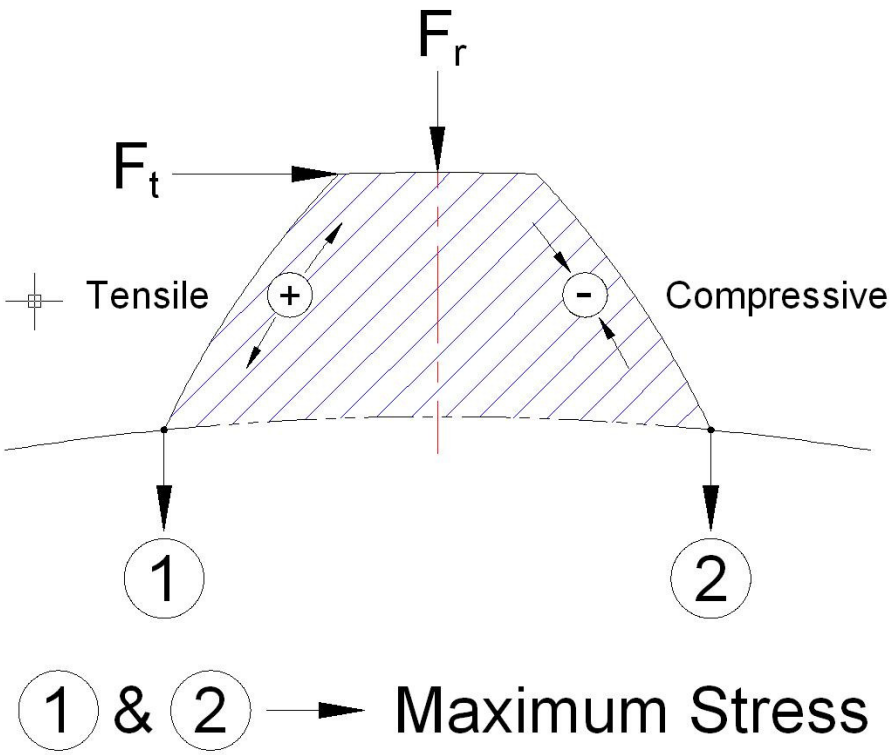

Figure 1. Tangential and Radial forces on gear tooth.

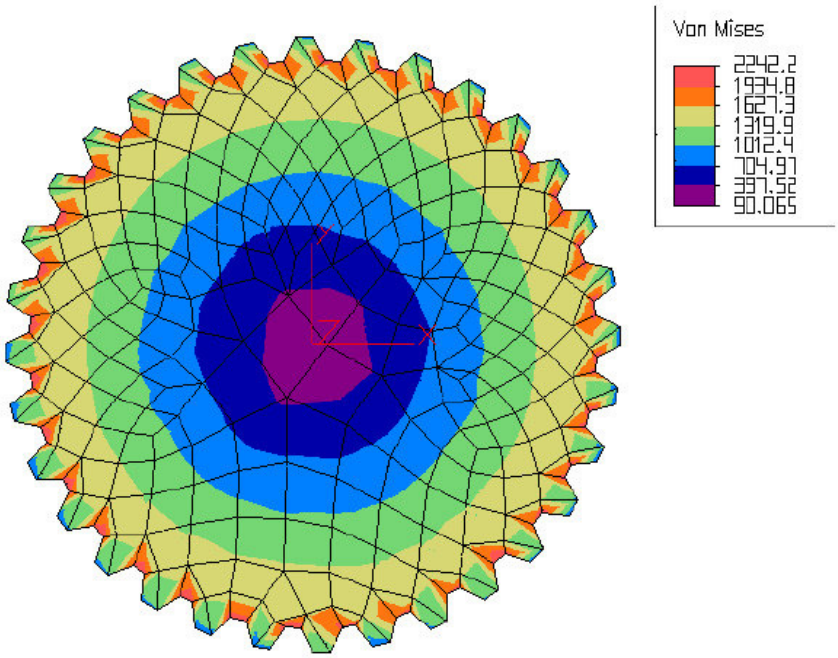

Figure 2. Involute Splines
Source; "Finite Element Study of Stresses in Stepped Splines and Partially Splined Shafts under Bending, Torsion and Combined Load" A Masters Thesis, Donald Alexander Baker (Virginia Tech).

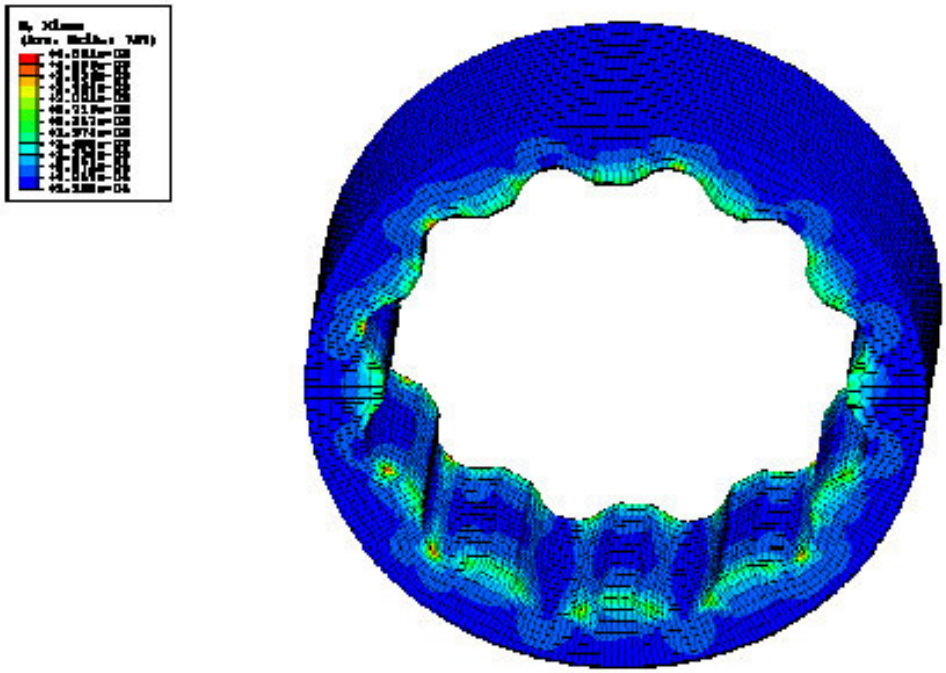

Figure 3. STEER's FEM analysis of Continua splines. (ANSYS 10)

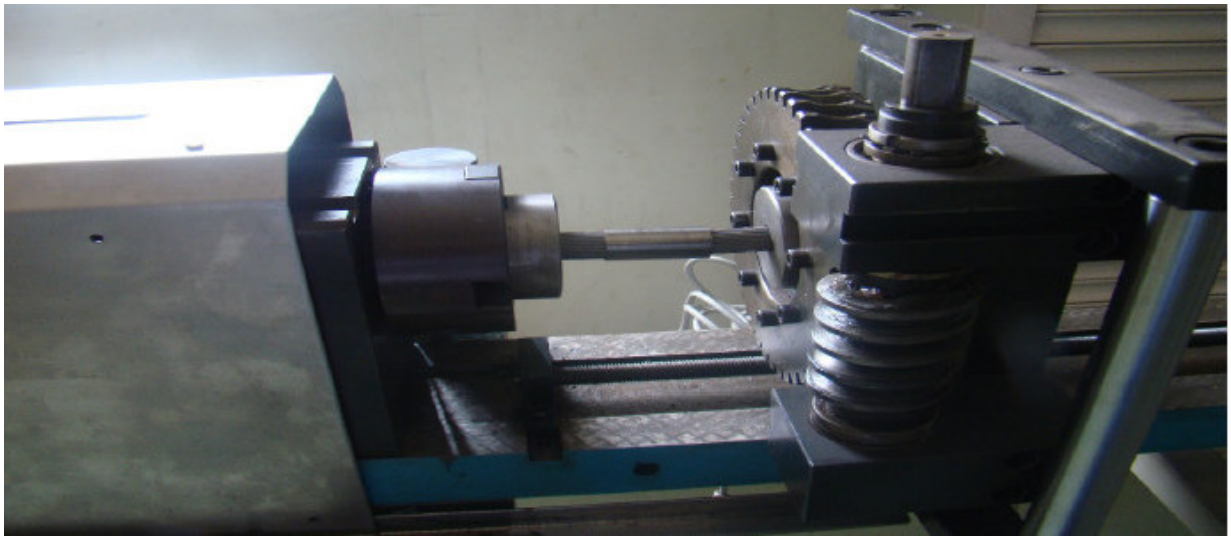

Figure 4. STEER's Torsional Test Rig.

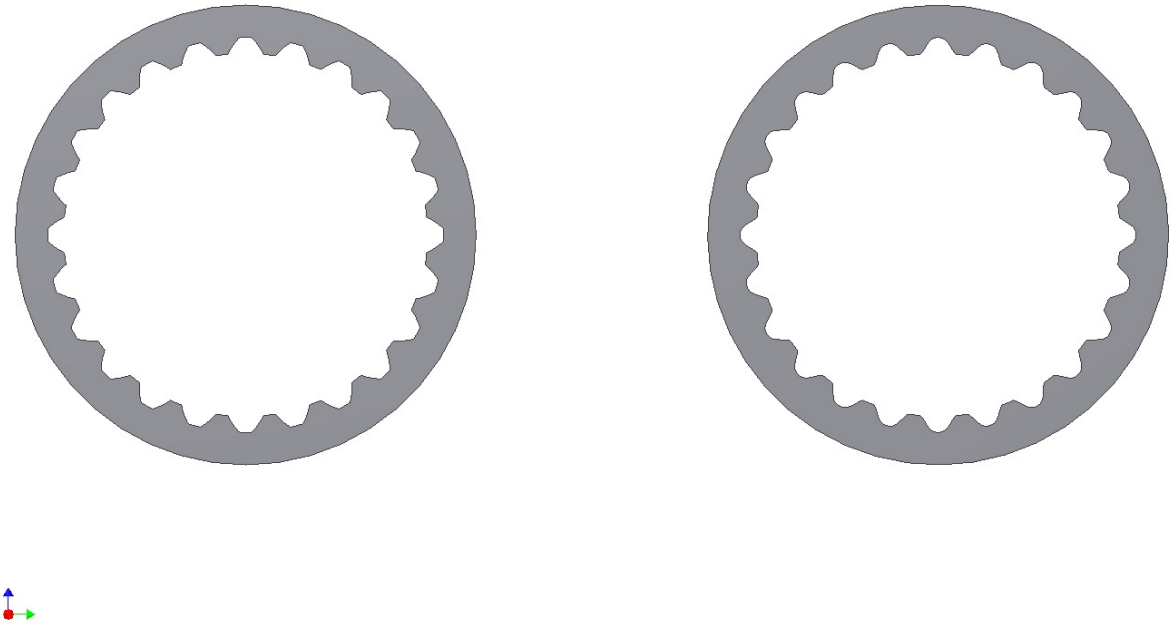

Figure 5. Involute and Continua cross sections of the bushings

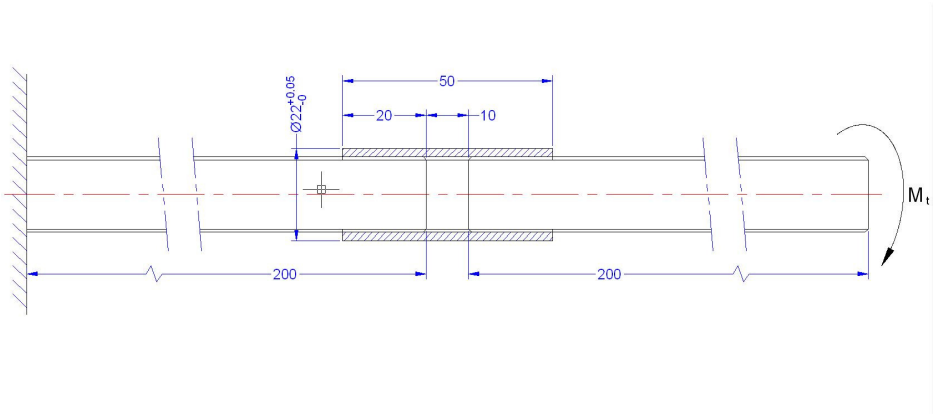

Figure 6. Experimental setup.

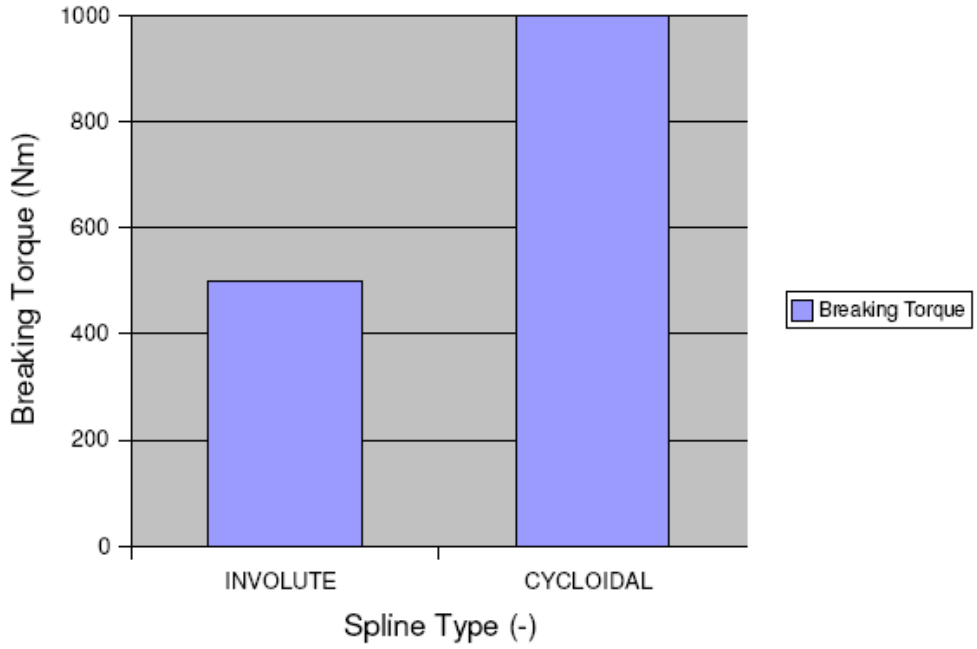

Figure 7. Torque Capacity results from TTR testing.

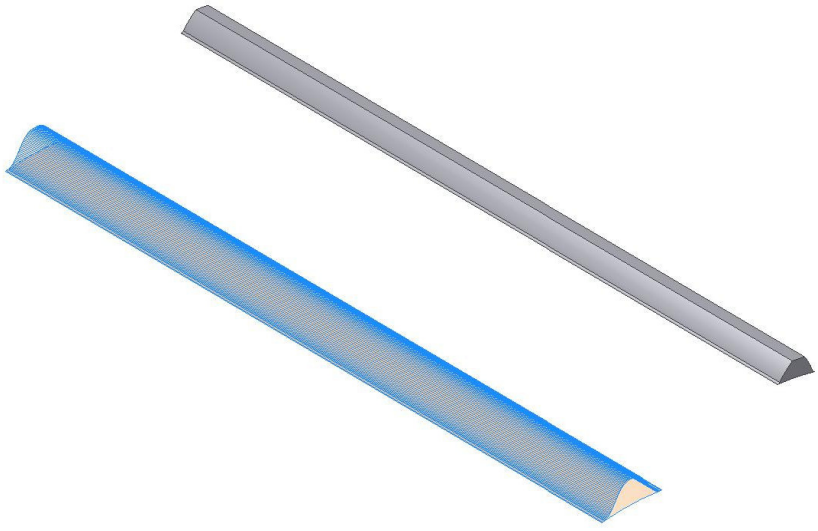

Figure 8. Spline morphology

Key words/ continua, spline, involute